



Fellenius, B.H., and Tan, S.A., 2012. Analysis of bidirectional-cell tests for Icon Condominiums, Singapore. Proceedings of the 9th International Conference on Testing and Design Methods for Deep Foundations, Kanazawa, Japan, September 18-20, 2012, pp. 725-733.

# Analysis of Bidirectional-cell Tests for Icon Condominiums, Singapore

Bengt H. Fellenius<sup>1)</sup> and Tan Siew Ann<sup>2)</sup>

<sup>1)</sup> Consulting Engineer, 2475 Rothesay Avenue, Sidney, British Columbia, V8L 2B. <Bengt@Fellenius.net>

<sup>2)</sup> Professor, Civil Engineering Department, National University of Singapore, 10 Kent Ridge Crescent, Singapore 119260. <ceetansa@nus.edu.sg>

**Keywords** Bored piles, bidirectional-cell, strain-gage records, pile bending, stiffness modulus,  $\beta$ -coefficient.

**ABSTRACT** Two 1,200 mm diameter bored piles were constructed for Icon Condominiums in Singapore and tested using a single bidirectional-cell level at the pile toe. The piles were about 23 m long and installed through 12 m of sandy silt deposited on a weathered siltstone bedrock (Jurong formation). Bending was evident at several gage levels. The records allowed an illustration of what appropriate decision to make when one gage of a pair is damaged, demonstrating the principle that if one gage is damaged, records from the surviving gage should be considered suspect, and, where two pairs are used, that the records of the surviving gage of the second pair must be discarded and not included in the average from the gage level.

The measurements showed the soil to be strain-hardening. Strain records from one gage level immediately above the pile toe showed large initial values which, at further loading, became moderate and similar to the development at other gage levels. The analysis of the data from that gage level indicated that the pile had been subjected to tension when cooling off from the high temperature induced during the concrete hydration, because the bedrock shaft resistance restricted the associated thermal contraction of the pile.

In the sandy silt, the shaft resistance distribution at the maximum test load was proportional to the effective overburden stress with a back-calculated proportionality coefficient,  $\beta$ , of about 0.7. Similarly, in the siltstone, the shaft resistance distributions correlated to a  $\beta$ -coefficient of about 2.0. The measured upward and downward load-movement data were fitted to q-w functions, i.e., t-z function for the shaft resistance and q-z function for the toe response. The so-fitted curves were used to produce an equivalent head-down load-movement curve and an equivalent resistance distribution with extrapolation to values beyond those imposed in the test. The equivalent head-down curves are used to illustrate the limitation of a conventional head-down test in that such tests do not explore the pile toe response as well as the bidirectional-cell test does.

## 1. INTRODUCTION

Two residential high-rise tower blocks were constructed in the western part of Singapore in November 2003 (Loadtest Asia 2003). The foundations were placed on 1,200 mm diameter bored piles constructed to depths ranging from about 20 to 25 m. To verify the design, bidirectional-cell static loading tests (Osterberg 1998) were conducted on two test piles instrumented with vibrating wire gages. This paper presents the results of tests on two test piles, Piles 1 and 2, constructed to embedment depths of 24.5 m and 22.4 m, respectively. The cell assemblies consisted of four cells and were placed 2.4 m and at 0.3 m above the toe in Pile 1 and Pile 2, respectively. This located the cell levels in the two test piles at almost the same depths, i.e., at 21.5 m and 21.7 m, respectively. The piles were supplied with eight and seven levels of strain-gage pairs, respectively. Broadly, the soil profile consisted of 12.5 m of clayey silt to sandy

silt (weak siltstone) deposited on dense to very dense silty sand to siltstone (Jurong Formation). The natural water content of the silty sand ranged from about 10 through 15 %. The depth to the groundwater table is not reported, but is assumed to be at 2.0 m depth, which is the same depth as that established in recent nearby previous projects in the Jurong formation. Figure 1 presents the soil profile and the schematics of the Pile 1 with the location of the strain-gage levels and cell assembly.

## 2. TEST PROCEDURE AND RESULTS

The testing procedure was a "quick test" with load increments applied every 15 minutes. Pile 1 was subjected to a single load cycle consisting of 35 load increments of 500 KN, whereas Pile 2 test included three loading events, the first two with 18 and 26 increments, respectively, and the third included 14 load increments.

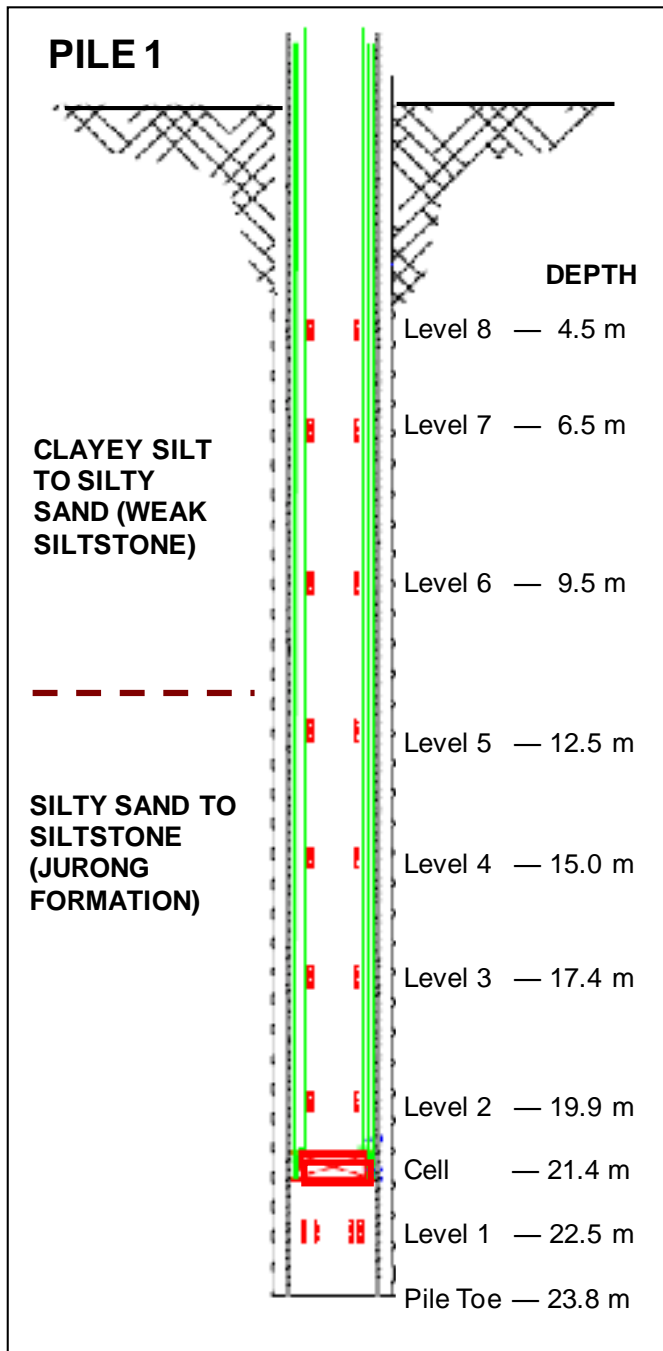


Fig. 1 Soil profile, test pile with strain gage and cell levels in Pile 1

Figure 2 shows the main load-movement data for the two tests. Pile 1 was tested to the maximum cell load available. The test on Pile 2 was limited by the limiting movement of the cell (the pile toe response of Pile 2 was less stiff than for Pile 1). The upward response is very similar for the two test piles. Although the maximum upward movements at the cell levels were 17 mm and 10 mm for Piles 1 and 2, respectively (the pile head movements were 14 and 8 mm), the curves show no tendency toward approaching ultimate resistance.

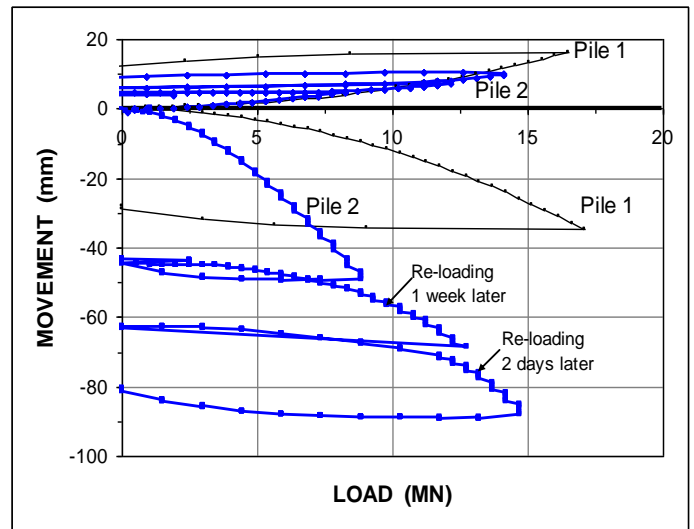


Fig. 2 Load-movement response of upper and lower cell plates for both test piles

As to the downward response, a question is whether the smaller downward stiffness shown by Pile 2 reflects a softer condition of the siltstone, or if it could be due to the proximity to the pile toe of the cell opening, 0.3 m above the toe. As the softer response is evident from the very start of the test, the latter cause is not probable.

Note also that despite the relatively large downward movement of Pile 2, the response does not show any tendency toward an ultimate value, confirming that toe bearing capacity is a delusion. Moreover, the two unloading/reloading events have not added anything of value to the test.

Figure 3 shows load-movements of Pile 1 cell opening ("expansion"). The records include the load-movements during the tack-weld breaking. The curve indicates that the pile was not subjected to residual load at the cell level. Neither does the similar plot for Pile 2 (not shown). The buoyant weight above the cell level for the piles was 600 kN.

### 3. STRAIN GAGE RECORDS

The strain-gage records from the tests are particularly interesting. Piles 1 and 2 were equipped with eight and seven gage levels, respectively. In both piles, two pairs (A&C and B&D) of vibratory wire gages were placed diametrically opposed at Gage Levels 1 and at Levels 7 and 8, respectively, while single pairs were placed at all intermediate levels. Figures 4A and 4B show the strains recorded by the individual gages and the average values

for Gage Pairs A&C and B&D at Gage Levels 1 in the piles. The single gages differ notably, but average values of the pairs are almost identical. The difference between the single gage records is considered due to influence of bending, causing the strains at the opposite sides of the pile to diverge.

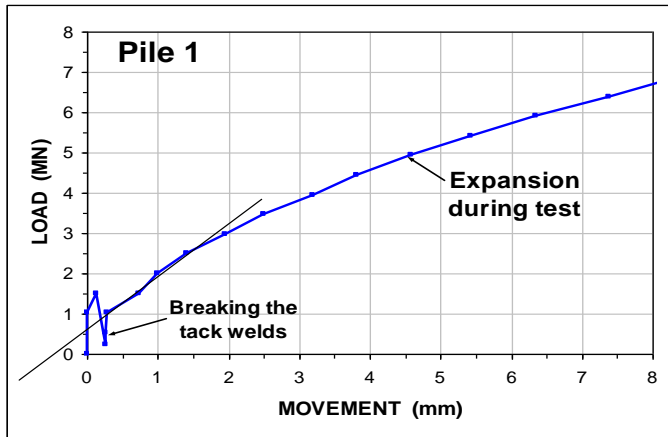


Fig. 3 Bidirectional-cell expansion in Pile 1

The records make for a very good example in support of the requirement that strain data must come from pairs of diametrically of gages, not from single gages. When two pairs of gages are used and one gage of one of the pairs does not work, practice often tends to take the average from all three surviving gages, not just from the two of the intact pair. Figure 5 demonstrates the folly of this approach in two curves from Level 1 in Pile 1 showing strain averages of three gages — each average being taken from one pair plus the records of a "surviving" gage, i.e., A&C+D and A&C+B. The reference is the average of all four pairs, A, B, C, D. It could be worse: if one gage of each pair had "died", then, to combine the two surviving gages, be it A&D or B&C, would entail an even larger error. Or, if only having one surviving gage, say, either D or B, which, as shown in Figures 4A and 4B, would be giving a wrong results and this at opposite sides of the spectrum despite that each single gage is functioning correctly.

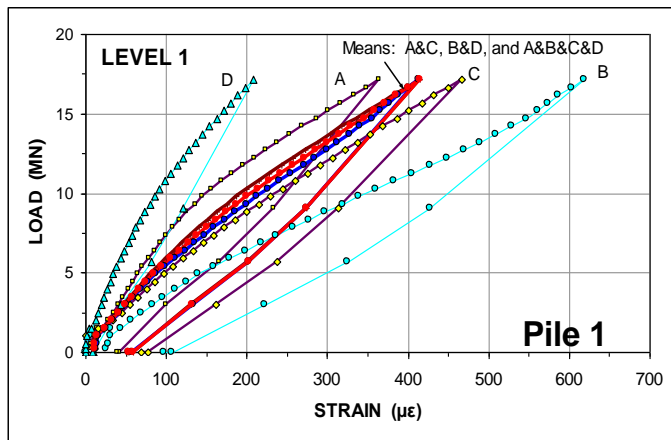


Fig. 4A Load-strain curves from Gage Level 1

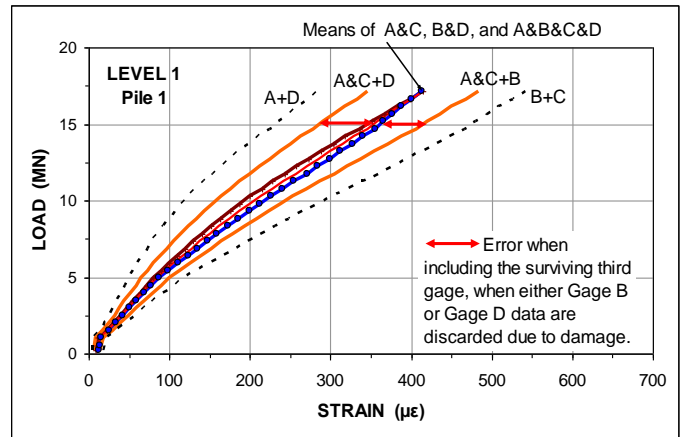


Fig. 5 Load-strain curves from Gage Level 1 in Pile 1

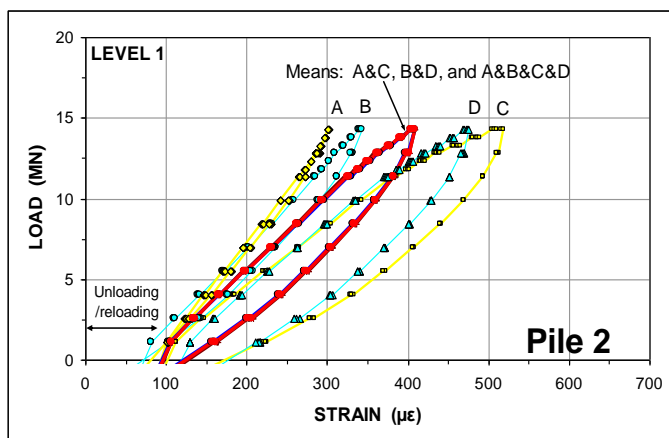


Fig. 4B Load-strain curves from Gage Level 1

The foregoing is further illustrated in Figure 6A through 6E showing the load-strain records in Pile 1 at Gage Levels 2 through 6. Although the strain curves from the individual gages at Levels 5 and 6 (Figures 6D and 6E) diverge considerably, the means of their values do not. The strains imposed at Levels 6 through 8 are not shown because they were smaller than  $10 \mu\epsilon$ , too small, to allow much inference from the values.

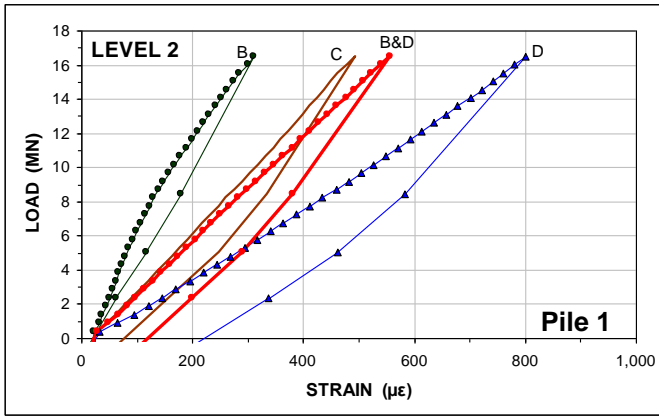


Fig. 6A Load-strain measured at Pile 1 Level 2

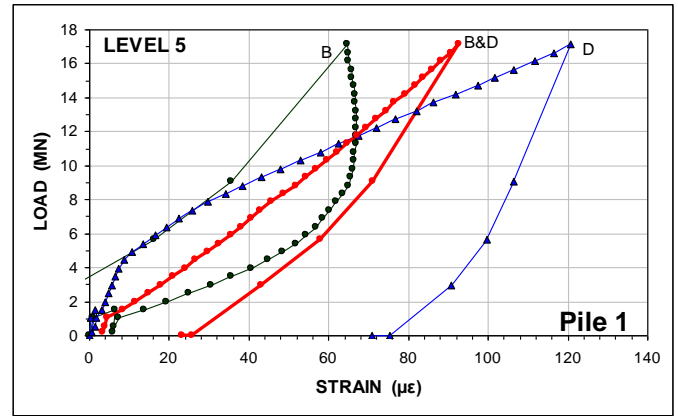


Fig. 6D Load-strain measured at Pile 1 Level 5

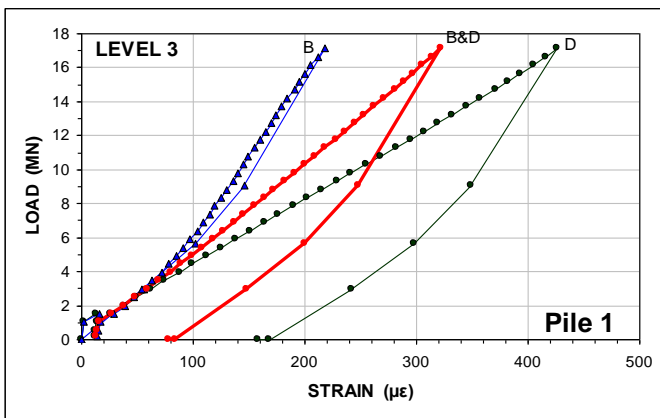


Fig. 6B Load-strain measured at Pile 1, Level 3

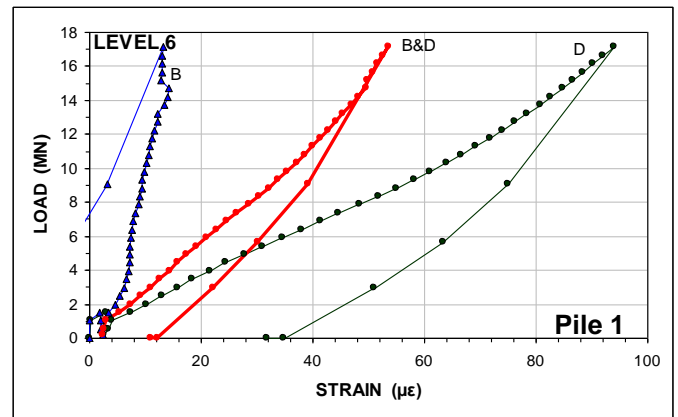


Fig. 6E Load-strain measured at Pile 1 Level 6

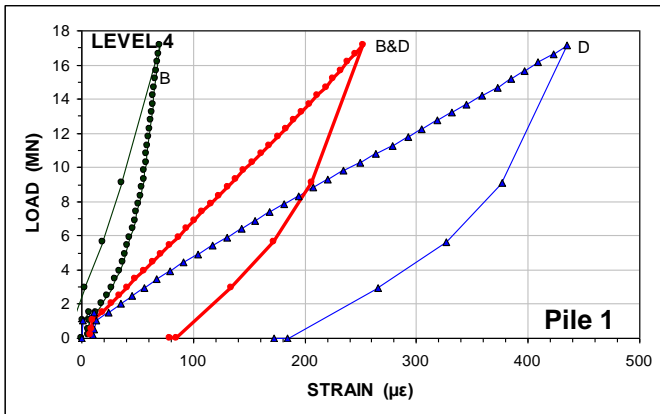


Fig. 6C Load-strain measured at Pile 1, Level 4

the figure. The slopes of Gage Levels 1 and 2 are reasonable for the size of the pile, but the slopes of Levels 3 through 5 are too steep, indicating a stiffness much larger than reasonable for the pile section. (Further discussed below).

#### 4. PILE STIFFNESS (MODULUS)

The average load-strain curves from the first five gage levels in Pile 1 are compiled in Figure 7. All show a practically straight line relation beyond strains of 100  $\mu\epsilon$  to 200  $\mu\epsilon$ . However, the slopes of the lines are different. The linear regression equations for the first four gage levels are shown in

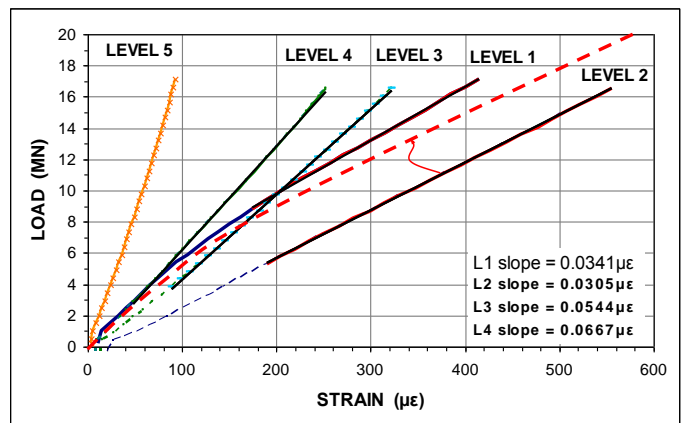


Fig. 7 Average load-strain lines for Gage Levels 1 through 5, Pile 1

Figure 7 indicates also an interesting observation pertaining to Gage Level 2, where the records of Gage Level 2 plot far to the right of Level 1

records. A location and a shape closer to that of the dashed red line would have been more reasonable. The reason is that the initial stiffness (below an imposed strain of  $200 \mu\epsilon$ ) is lower than the stiffness later in the test. It is most probable that the pile has experienced tensile fracturing during the concrete hydration at the Gage Level 2, when, first, the initially moldable wet concrete mix heated up and, subsequently, the hardened concrete cooled (Fellenius et al. 2009). The rise of temperature in a bored pile due to the hydration process usually ranges from  $60^\circ\text{C}$  through  $80^\circ\text{C}$ , but it can on occasion be even higher. The cooling to soil temperature caused shortening of the pile (and also of the width, but the latter only acts across the diameter, whereas shortening accumulates along the full pile length). Then, wherever along the pile, the shaft resistance is able to prevent the pile from reducing in length due to the thermal contraction, the pile is subjected to tension. Occasionally, the tension is large enough to cause fissures in the pile.

The conclusion that tension has developed at Gage Level 2 to the point of causing fissures in the pile, is supported by the fact that, after breaking the tack weld and unloading the cell assembly, the Level 2 gage showed a net shortening of  $20 \mu\epsilon$ , two to three times as much as that recorded for Gages L1 and L3. When the test commenced, the initial load increments were transferred mainly through the reinforcement, which resulted in larger shortening (larger strain values) than had the concrete been fully engaged. Progressively, also the concrete became activated, but the full pile section was not engaged until the imposed strain was about 100 to  $200 \mu\epsilon$  after which the stress-strain relations became linear (cf. Figure 7). Because of the initially imposed overly large strain, the total strains measured cannot directly be used to determine the load at Level 2. The values would show a too large load. It appears probable that the closing of the fractures gave an additional at least  $70 \mu\epsilon$  over and above the initial  $20 \mu\epsilon$ , and, therefore, the loads are calculated after subtraction of  $100 \mu\epsilon$  from each value of total strain measured. A value of  $100 \mu\epsilon$  over a 3 m length corresponds to 0.3 mm shortening. For a discussion of the phenomenon of fissures developing in the hydration process, see Sinnreich (2012).

A more detailed resolution of the pile stiffness for Gage Levels 1 and 2 is obtained in a "tangent modulus" ("incremental stiffness") plot shown in

Figure 8. The plot shows the incremental stiffness to be practically constant with increasing strain. The stiffness equation shown gives the linear regression stiffness (AE) for Gage Level 2. A stiffness value of 30.5 GN for the nominal cross section (concrete and reinforcement) of the pile correlates to an E-modulus of 26.5 GPa for the concrete.

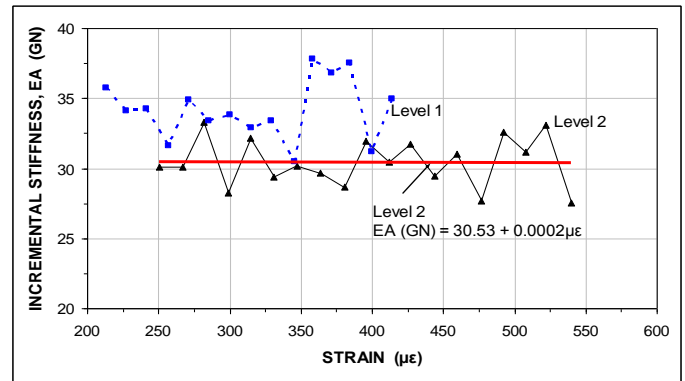


Fig. 8 Incremental stiffness plot of records from Levels 1 and 2, Pile 1

Before the ultimate shaft shear is reached, the increasing load will result in progressively increasing strain. Eventually, for materials having constant E-modulus or a linear relation between modulus and imposed strain, and provided the soil response goes into plastic state — ultimate shaft resistance — the ratio between load increment and strain increment becomes constant, manifested in a linear load-strain curve and a constant incremental stiffness because, once the state is plastic, all applied new increments of load will travel up or down the pile unreduced by shaft resistance. However, to develop the linearity, the total movement needs to be quite large so that several readings can be taken before the pile shaft plunges and the test is finished. This means that, normally, the stiffness can only be observed for gages close to the load source, such as near the pile head in a head-down test or near the cell in a bidirectional test. It also means that a test should be designed for several small increments of load rather than a few large increments.

Once the ultimate shear resistance has been reached at a gage level, further load increases and associated strain increases will reflect the true stiffness of the pile at the gage level. The stiffness is the slope of the load-strain curve or of the incremental stiffness curve. When the shaft resistance has reached a plastic state with neither strain-hardening nor strain-softening the linear slope represents the modulus of the material.

However, if the soil response at large shaft movement is not plastic, but strain-hardening, then, each load increase reaching the gage level will be smaller than the increment of the applied load and the induced strain correspondingly smaller than that for when the load increase at the gage level is equal to the applied load increment. Even if then the strain-hardening soil shear is an approximately linear function of the movement, the slope of the line does not then represent the stiffness of the material., but a larger stiffness than the true value will be inferred, as is demonstrated by Gage Levels 3 and 4 in Figure 7, which showed stiffness (i.e., slope of the curve) larger than that shown for Gage Levels 1 and 2, implying influence of strain-hardening. The observation may be due to true soil hardening and/or due to protrusions of the pile gradually engaging the soil as the pile shaft moves.

Moreover, because of the strain-hardening, the loading test can be carried out to larger shaft movement than would be possible had plastic shaft shear response been the case.

The strain values measured by Gage Level 2 were considered representative for the pile material. They were converted to load through the relation for constant stiffness,  $AE$ , of 30.5 GN (Figure 8). The relation was also applied to the strain values at Gage Levels 2 through 4. The so-determined load values were then differentiated to show the percent increase of load for each increment of load, which results are shown in Figure 9.

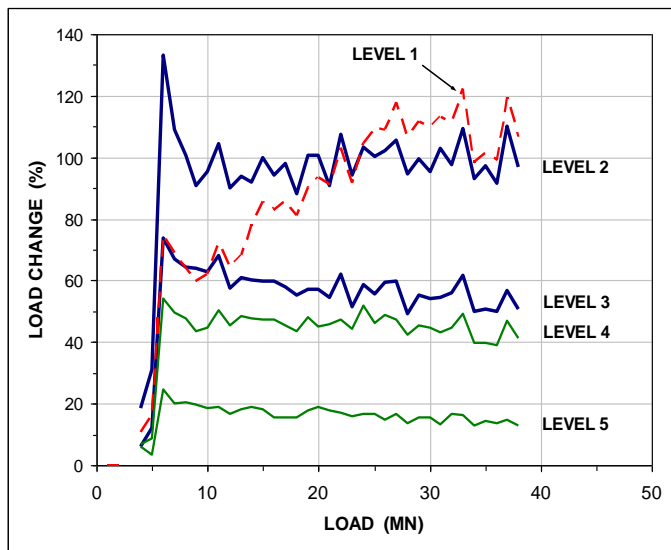


Fig. 9 Differentiated load increase at each gage level in ratio to the incremental load increase

If, as is often the case, the shaft resistance values reach an ultimate value and do not show appreciable increase for further movement — ultimate resistance reached — the differentiated load increase will be equal to the actual load increase (in the cell), as is indicated for Gage Level 2, Figure 9, where the incremental increase of load is about equal (100 %) to the applied load increment. At the other gage levels, each increase beyond a total load of about 10 MN is of about the same size each other, but significantly smaller than the applied load increment. This means that the shaft shear near Gage Level 2 has a plastic response, while at Gage Level 3 the response is strain-hardening. The response at Gage Level 4 is affected by the load response at Gage Level 3 and, therefore, whether or not it also is strain-hardening is not definite. The strain hardening response explains why the test could impose a movement as large as 15 mm without the pile shaft experiencing plunging failure. (A strain softening would have shown differentiated values larger than the applied load increments and the test would have plunged long before the movement could have reached 15 mm).

## 5. LOAD DISTRIBUTION

Figure 10 shows calculated strain-gage load values plotted against measured movement. The reasonably smooth curves indicate that the data are of good quality.

The evaluated strain-gage loads are plotted versus depth in Figure 11. Note that the load distribution shown between the cell and the Gage Level 3 locations is about the same as if the Gage Level 2 records had been disregarded. The main point made is that the vibratory wire gages at Gage Level 2 are functioning well and the seemingly erroneously large strains are due to closing of tensile fissures in the initial stage of the test, not to malfunctioning gages.

Figure 12 shows the average shaft resistance as mobilized along the pile between each gage level as the test progressed. The column marked "β" compiles values of the ratio between the at-end-of-test load difference between the gage levels divided by the shaft area and the mean effective stress between the gage levels. The average β from the cell up to Gage Level 5 is 2.0. The actual values

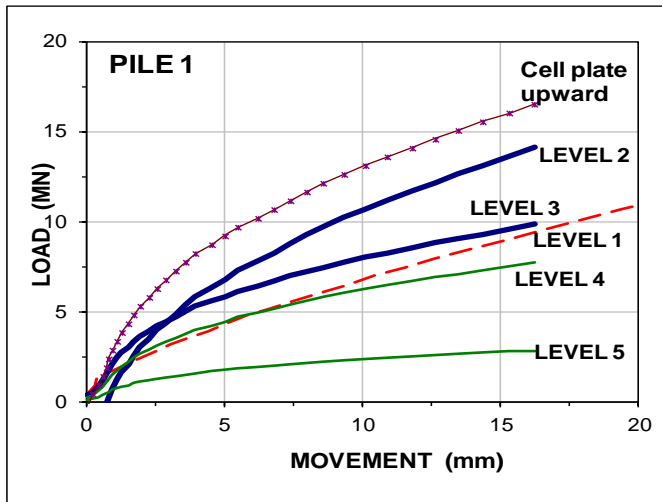


Fig. 10 Calculated strain-gage load values plotted against measured movement

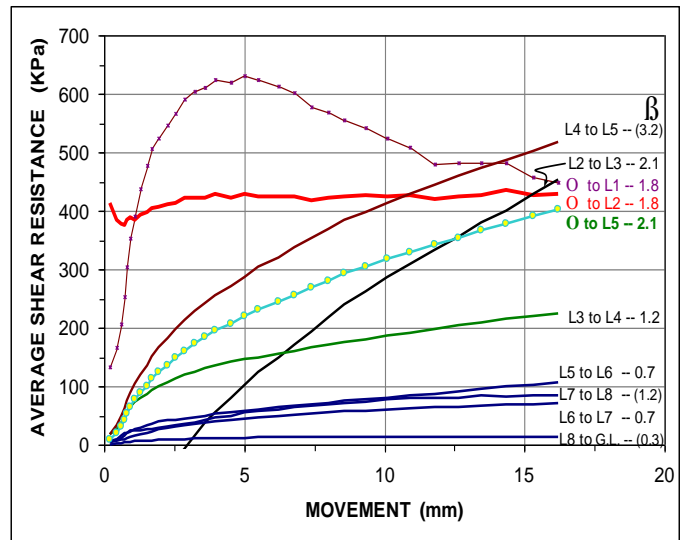


Fig. 12 Pile 1 Average shaft resistance between gage levels

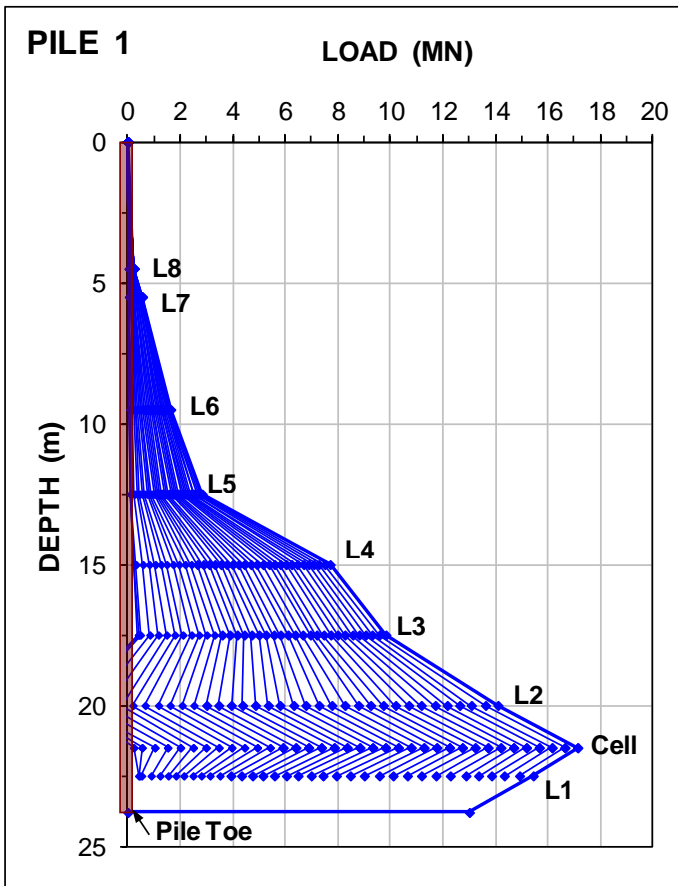


Fig. 11 Pile 1 load distributions

of the individual curves, albeit not the shape of the curves, are very sensitive to small variations of the evaluated pile stiffness relation. Therefore, the values of the  $\beta$ -coefficients are somewhat approximate.

Figure 12, confirming the conclusions drawn from Figures 7 and 9, indicates that the shaft shear response between the cell and Gage Level 2 was neither strain-hardening nor strain-softening. Above Gage Level 5, moderate strain-hardening is indicated. However, between Gage Levels 2 and 3, 3 and 4, and 4 and 5, respectively, the response is clearly strain-hardening, although between Gage Levels 3 and 4, the strain-hardening response appears to be less pronounced. Small adjustments to the assumed stiffness value would make the three curves to plot closer to each other. The results indicate that the siltstone demonstrates a strain-hardening response throughout the length from Gage Levels 2 through 5.

The shape of the curve from cell to Gage Level 1 is probably influenced by interaction between shaft shear and toe resistance and/or the opening of the cell and cannot be taken as showing a strain-softening response.

## 6. EQUIVALENT HEAD-DOWN CURVES

Figure 13 shows the distributions of Figure 11 together with the distribution for an equivalent head-down test carried out to a pile head load equal to twice the cell load. That is, the curve for the last upward distribution is "flipped over" so as to show the cell shaft resistance as positive direction resistance instead of negative (Fellenius 1989, 2011). The toe resistance value is an extrapolation of the trend from the cell over the load at Gage Level 1.

Figure 13 also shows a plot of the calculated load distribution fitted to the strain-gage values in an effective stress analysis. The average back-calculated  $\beta$ -coefficients are 0.7 in the silty sand layer and 2.0 in the siltstone, agreeing well with the values determined from the load differences between the individual gage levels.

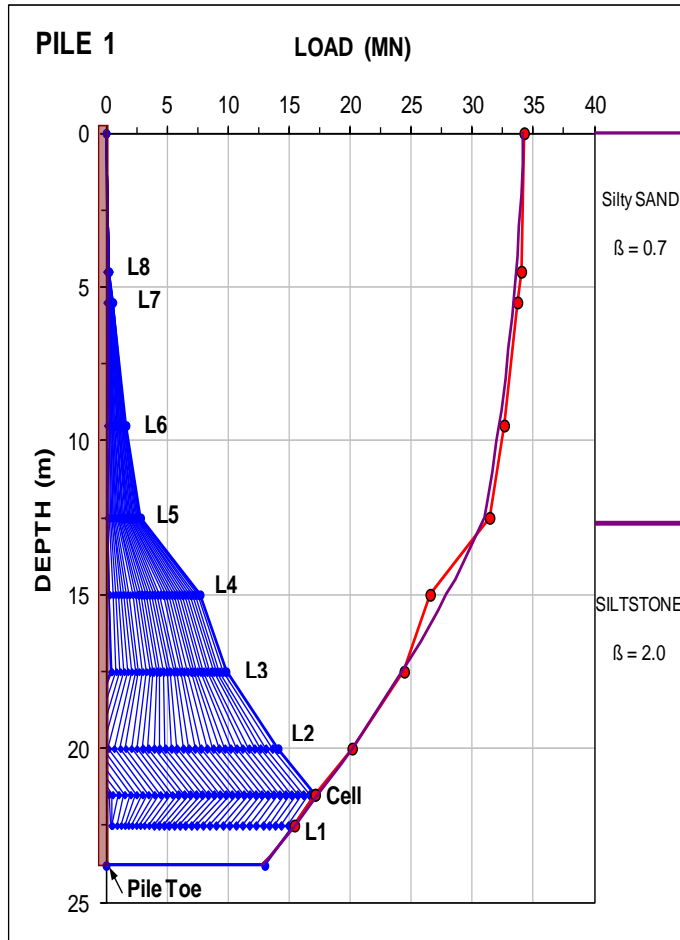


Fig. 13 Load distribution of Pile 1 test and for its equivalent head-down test

The equivalent head-down load-distribution diagram is a useful reference to the results of a conventional head-down test. A second type of equivalent head-down curve, routinely provided in reports of bidirectional-cell test results, can be developed from the load-movement measurements of the cell plates. The curve is constructed from combining the upward and downward load at equal movements with adjustment to the larger pile compression obtained in a head-down test as opposed to a bidirectional-cell test. Where the maximum upward and downward movements are unequal (almost always the case), the curve that is "short" can be extrapolated by a hyperbolic fit or a

$t$ - $z$  or  $q$ - $z$  function fit (Fellenius 2011). Figure 14 shows the results of extrapolations fitted to the upward test curve: i.e., shaft resistance, only, as measured and as fitted to two  $t$ - $z$  curves.

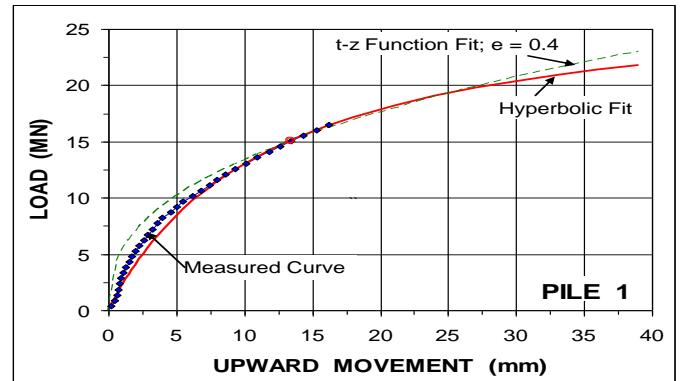


Fig. 14 Measured and fitted load-movement curves for the Pile 1 upward results

Figure 15 shows simulated head-down load movement curves for Pile 1 developed using  $t$ - $z$  and  $q$ - $z$  functions fitted to the upward and downward test measurements together with one obtained directly from the test data and by the shaft response determined by hyperbolic fitting to the shaft response and used to extrapolate the curve beyond the maximum upward shaft movement. Two important points are indicated on the curves. The first point denotes where in the simulated head-down test the movement calculated for the depth of the cell (21.5 m) is equal to the maximum measured upward movement (15 mm). The second point shows where the movement calculated for the depth of the pile toe (24.5 m) is equal to the cell measured maximum downward movement (34 mm).

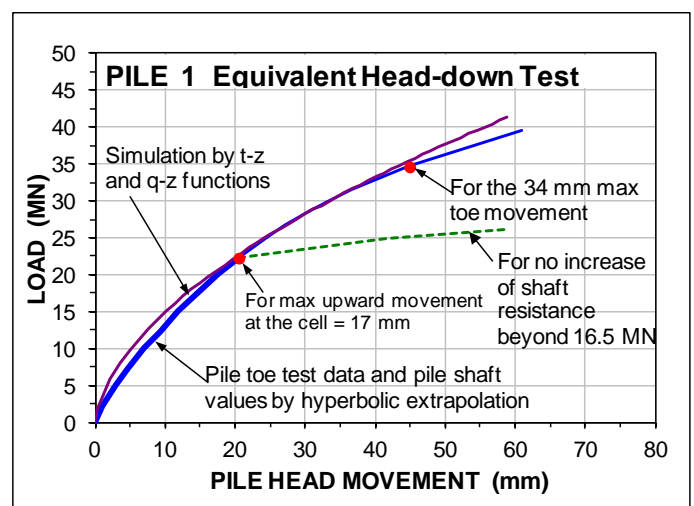


Fig. 15 The equivalent head-down load-movement curves of Pile 1 test.

The curve dashed beyond measured maximum upward movement shows where the shaft resistance is equal to the test value (16 MN). From then on, the gain shown by the dashed curve for increasing movement is from toe resistance only, which is a conservative assumption. The simulated curves beyond a movement of the maximum measured toe movement are extrapolations to illustrate a tendency.

The curve marked "... values by hyperbolic extrapolation" is the curve shown in the routine field report (Loadtest Asia 2003). The curve marked "Simulation by t-z and q-z functions" has been calculated using the UniPile software (Fellenius and Goudreault 1998) assuming t-z and q-z relations, a pile E-modulus of 26.5 GPa ( $AE = 30.5 \text{ GN}$ ) in an effective stress analysis with  $\beta$ -coefficients as shown in Figure 13, and a groundwater table located at a depth of 2.0 m with hydrostatically distributed pore pressure.

Singapore practice employs an acceptance criterion for the working load applied to a pile as the load for which the test shows a pile head movement of 25 mm for a load equal to twice the working load. The criterion applies also to the equivalent head-down test determined in a bidirectional-cell test. At a pile head movement of 25 mm, the applied load ranges from 22 MN through 27 MN, depending on whether or not the shaft resistance is assumed to continue to increase. The working load based on the Pile 1 test results would be half this load range, i.e., range from 11 MN through 13.5 MN.

In order to stay within the assigned length of the paper, the results of the test on Pile 2 are not included. As indicated in Figure 2, the Pile 2 test was stopped short of the maximum upward load of Pile 1 and showed a less stiff toe response. However, a similar shaft resistance strain-hardening effect was established. Had the Pile 2 test continued to an upward shaft movement similar to that for Pile 1, it is evident that the shaft resistance distribution for the two piles would have been very similar.

Figure 16 shows the equivalent head-down curves fitted to t-z and q-z functions and applying the same exponents, 0.4 and 0.6, and the actual values of load at the maximum shaft and toe displacements measured in the tests for Piles 1 and 2, 17 mm and 9 mm, and 34 mm and 85 mm, respectively.

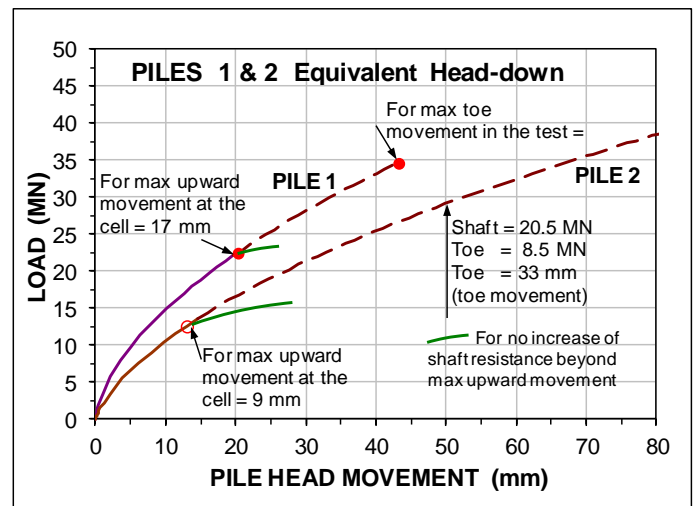


Fig. 16 Equivalent head-down load-movement curves of Piles 1 and 2

The two test piles show markedly different toe response to the applied test loads, while yet having very similar shaft responses. It is quite probable that the construction of Pile 2 left the pile toe with some debris at the bottom of the shaft resulting in the soft toe response. This is frequently experienced when constructing bored piles in Singapore (Fellenius and Tan 2010, Tan and Fellenius 2012).

In evaluating the results of a static loading test, extrapolated values must be given less credence, or weight, than measured values. That is, in terms of a factor of safety, a larger factor is required for an extrapolated relation, such as the portion of the equivalent load-movement curves beyond the maximum shaft resistance in Figure 16. The dashed portions of the curves continue the shaft resistance strain-hardening trend, whereas the differently shaded portions breaking off toward larger movements assume plastic shaft resistance response, both curves employing actually measured toe resistance.

The analysis of the results of the test on Pile 2 is adversely affected by the unloading/reloading events. Each such event locks in stress in the pile and shear forces in the soil and changes the stiffness response of the system for the continued test, as well as the construction of the equivalent head-down load-movement curve. There is no offsetting benefit to the test of such cycles of load.

A detailed numerical study of the Pile 1 test data has been presented by Bui et al. (2005).

## 7. CONCLUSIONS

1. The analysis of the vibrating-wire strain-gage data showed all individual gages to function properly. The strain records showed the pile to be influenced by bending and that, therefore, the measured strains differed across the pile diameter. Gage Levels 1, had two pairs of gages and the records showed that the mean of both pairs were equal, whereas the individual gage records differed significantly. The records demonstrate the important fact that when one gage of a pair does not function, the measured values of the surviving gage records must be abandoned.
2. The strain-gage records were used in an incremental stiffness (tangent-modulus) analysis to evaluate the pile stiffness, EA, which was determined to be practically constant with increasing load and strain with a value of 30.5 GN for the pile section corresponding to an E-modulus of 26.5 GPa for the concrete.
3. The analysis indicated that Pile 1 had been subjected to tension at the gage level closest to the bidirectional-cell, when cooling off from the high temperature induced during the concrete hydration, due to the bedrock shaft resistance restricting the thermal contraction of the pile. The thermal contraction resulted in fissures, which had to be closed before the full concrete could start reacting to the imposed stress over the full pile cross section. The reduction of the thermal contraction as recorded by the Level 2 strain-gages was about 100  $\mu\epsilon$  additional strain.
4. The analysis shows that the shaft resistance along the pile is strain-hardening, which is the reason for why the shaft resistance continued to increase even after a relative movement as high as 17 mm at the bidirectional-cell level and 15 mm at the pile head (Pile 1).
5. The analyses also showed that at the maximum shaft movement, the distribution of shaft resistance correlated to effective stress proportionality coefficients,  $\beta$ , equal to 0.7 and 2.0 in the upper about 12 m of soil, a silty sand, and in the lower siltstone (Jurong Formation) below, respectively.
6. The bidirectional-cell tests showed that the shaft responses of the two test piles were very similar,

but the toe responses were quite different. The Pile 2 toe response was much less stiff than that of Pile 1. It is probable that the construction left Pile 2 with some debris at the bottom of the shaft. The consequence of the smaller stiffness is particularly obvious in the evaluation of the test results in terms of equivalent head-down load-movement curves.

7. Pile 1 was tested in one continuous loading event. In contrast, Pile 2 was subjected to three cycles of loading, which considerably impaired the quality of the test for detailed analysis.

## ACKNOWLEDGEMENTS

Permission by Loadtest Asia Pte. Ltd. to present the analysis of the case data is gratefully acknowledged.

## REFERENCES

- Bui, T.Y., Li, Y., Tan, S.A. and Leung, C.F., 2005. Back analysis of O-cell Pile Load Test using FEM. Proc. of the 16th ICSMGE, Osaka Sep. 12-16, Millpress Science, pp. 1959-1962.
- Fellenius, B.H., 1989. Tangent modulus of piles determined from strain data. The ASCE Geotechnical Engineering Division, 1989 Foundation Congress, Edited by F.H. Kulhawy, Vol. 1, pp. 500-510.
- Fellenius, B.H., 2011. Basics of foundation design, a text book. Revised Electronic Edition, [www.Fellenius.net], 374 p.
- Fellenius, B.H. and Goudreault, P.A., 1998. UniPile Version 3.0 for Windows. Users Manual, UniSoft Ltd., Ottawa, [www.UnisoftLtd.com]. 64 p.
- Fellenius, B.H., Kim, S.R., and Chung, S.G., 2009. Long-term monitoring of strain in instrumented piles. ASCE Journal of Geotechnical and Geoenvironmental Engineering, 135(11) 1583-1595.
- Fellenius, B.H., and Tan, S.A., 2010. Combination of O-cell test and conventional head-down test. ASCE Geot. Special Publ. M.H. Hussein, J.B. Anderson, and W.M. Camp, Ed. GSP198, pp. 240-259.
- Loadtest Asia Pte. Ltd. 2003. Report on Drilled Pile Load Testing Osterberg method for Icon Condominiums, Singapore (LTA-3012-1 and LTA-3012-2). 194 p.
- Osterberg, J.O. 1998. The Osterberg load test method for drilled shaft and driven piles. The first ten years. Deep Foundation Institute, 7th Int. Conf. a. Exhibit on Piling and Deep Foundations, Vienna, Austria, June 15-17, 1998, 17 p.
- Sinnreich, J. 2012. Strain Gage Analysis for Nonlinear Pile Stiffness. Geotechnical Testing Journal, ASTM International, 35(2) 1-10.
- Tan, S.A. and Fellenius, B.H., 2012. Failure of a barrette as revealed in an O-cell test. ASCE Geot. Special Publ., M.H. Hussein, R.D. Holtz, K.R. Massarsch, and G.E. Likins, eds., GSP 227, pp. 307-321.